EARTHQUAKE ENGINEERING AND STRUCTURAL DYNAMICS, VOL. 21, 127–144 (1992)

THE SYSTEM DAMPING, THE SYSTEM FREQUENCY AND THE SYSTEM RESPONSE PEAK AMPLITUDES DURING IN-PLANE BUILDING–SOIL INTERACTION

M. I. TODOROVSKA* AND M. D. TRIFUNAC†

Department of Civil Engineering, KAP 210, University of Southern California, Los Angeles, CA 90089-2531, U.S.A.

SUMMARY

The system damping, the system frequency, the relative building response and the base rocking response peak amplitudes are studied, as those depend on the building mass and height, the flexibility of the soil, the structural damping, the type of incident waves and their angle of incidence. A linear two-dimensional model is used, which assumes the soil to be a homogeneous isotropic half-space, the foundation supporting the building to be a rigid embedded cylinder, and in which the building model is an equivalent single-degree-of-freedom oscillator. The system frequency and the system damping ratio are determined by measuring the width and the frequency of the peak in the transfer function of the oscillator relative response, using the analogy with the half-power method for a single-degree-of-freedom fixed-base oscillator. Previous similar studies are for dynamic soil–structure interaction only, and for simplified models in which the stiffness of the soil and the damping due to radiation are represented by springs and dashpots. The study in this paper differs from the previous studies in that the wave passage effects (or the kinematic interaction) are also included, and that no additional simplifications of the model are made. Results are shown for excitation by plane P- and SV-waves.

INTRODUCTION

Studies on dynamic soil–structure interaction have shown that the transfer function of the motion of a building on a flexible foundation medium may differ significantly from the transfer function of the motion of a fixed-base model. The interaction introduces 'damping' because of the radiation of the building energy into the soil, and, so, the relative building response is bounded even in models without structural damping. The system frequency, the system damping and the relative building response, associated with the fundamental mode of vibration, are affected most. The frequency of the first peak of the transfer function (between the relative building response and the incident wave motion) is lower than the fundamental natural frequency of the fixed-base model.

The system damping and the change of the system frequencies, during dynamic soil–structure interaction have been studied by several authors[2–5,7,8] using some analogy with a single- or a multi-degree-of-freedom (SDOF and MDOF) fixed-base oscillator. Bielak[2] and Luco[5] presented simple analytical expressions for the modal damping ratios, the system frequencies and the peak responses for SDOF and MDOF building models on a flexible foundation medium, by neglecting the higher order terms of the functions expressing the damping coefficients. In his later work Bielak[4] arrived at similar analytical expressions assuming that the modes of the flexible base structure are orthogonal. Tsai,[8] assuming orthogonal modes of vibration of the flexible base building, calculated the damping for each mode by matching the shape of the transfer function of his model with the 'actual' transfer function at several locations along the height of the building. Rainer[7] calculated the total damping for SDOF and MDOF building models (i) measuring the amplitude of the relative building response transfer function at the fundamental system frequency and (ii) from the ratio of the

*Research Associate.
†Professor.

0098-8847/92/020127-18$09.00
© 1992 by John Wiley & Sons, Ltd.

Received 11 February 1991
Revised 20 August 1991

energy dissipated during one cycle and the total potential energy during one cycle, associated with a particular mode of vibration. The system response during dynamic building–soil interaction, for buildings on a prismatic embedded foundation, has been studied by Bielak.[3] In all of these models, the stiffness of the soil and the damping via radiation are represented by a pair of a spring and a dashpot for each degree of freedom of the foundation, and the excitation is a horizontal driving motion with constant amplitude.

In this paper, the system frequency, the system damping ratio, the peak relative building response and the peak base rocking response during building–soil interaction are studied, as functions of the flexibility of the soil, of the structural damping ratio, of the building mass, of the type of incident waves and of the angle of incidence. Besides the dynamic (inertia) interaction, the kinematic interaction (wave passage effect) is also included. The effects of the scattering and diffraction of the incident waves from the building foundation on the system damping, during building–soil interaction, have not been studied so far. One of the aims of this study is to see under which conditions these effects are significant.

Incident plane P- and SV-waves are considered in this study. Because the first mode contributes most to the building response, in this analysis, the contribution of the higher modes is neglected. In the two-dimensional model used, the building is represented by a single-degree-of-freedom equivalent oscillator supported by a circular foundation embedded into a homogeneous elastic half-space. The material damping in the soil is ignored. The analysis is linear and the substructure approach is used. The model is analytical and allows closed-form solutions for the motions of the building base and for the relative response. The analytical expressions for the foundation impedance matrix and the foundation driving forces for this model have been derived by Todorovska and Trifunac,[10] in their study of soil–structure interaction for a shear wall for incident plane P- and SV-waves and for surface Rayleigh waves. Their two-dimensional model has been chosen in this study because it allows analytical closed-form solutions, and, therefore, better and more explicit understanding of the interaction phenomena.

With the current developments in numerical modelling of the foundation impedance functions, it is becoming possible[1,6] to consider irregular three-dimensional embedded foundations in a visco-elastic layered half-space, and to postulate different damping mechanisms in the soil surrounding the foundation. As these numerical models are further refined, it is becoming essential to establish some reference cases, for relative comparison with simple analytical solutions, which have been developed under controlled and easily understood conditions. One aim of this work is to contribute one such analytical solution.

The energy dissipated via scattering and diffraction from the building foundation should be studied more explicitly, and in the absence of other dissipation mechanisms, so that we can understand its full potential for reducing the relative response amplitudes. In this paper, we characterize this dissipation via a simple analogue of viscous damping, measured by the width of a SDOF relative response peak, and show how it depends on all other system parameters.

THE MODEL

In the model, shown in Figure 1, the building is represented by a single-degree-of-freedom (SDOF) equivalent oscillator supported by a rigid circular foundation embedded into a homogeneous elastic half-space. The half-space has shear modulus μ, shear wave velocity β, Poisson's ratio ν and no material damping. The oscillator consists of a rod which at one end has a concentrated mass, and at the other end is connected to the foundation, at point O, through a rotational spring and a rotational damper, connected in parallel. The mass per unit length in the y-direction of the oscillator is m_b. It has height H and radius of gyration r_b. The rotational spring has stiffness K_b, and the dashpot has damping constant C_b. The foundation has width $2a$, depth h and mass m_f per unit length in the y-direction.

The x–0–z coordinate system is an inertial system with origin at the centre of the top surface of the foundation at rest. The foundation has three degrees of freedom with respect to this coordinate system: horizontal translation Δ (in the positive x-direction), vertical translation V (in the positive z-direction) and rotaion φ (clockwise). The building model has only one degree of freedom with respect to the foundation—the rocking angle ψ^{rel} measured clockwise from the axis ξ, which is always perpendicular to the top surface of the foundation. With respect to the inertial system x–0–z, the centre of mass of the oscillator has

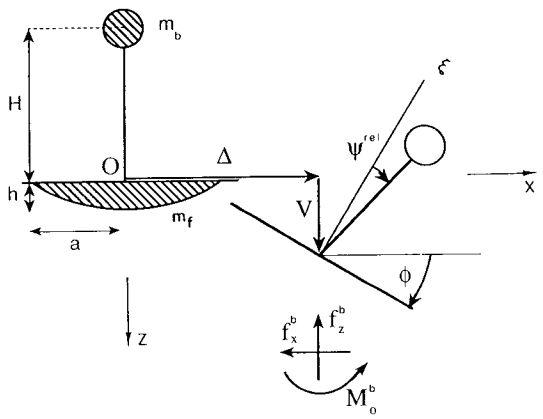

Figure 1. The model

horizontal displacement u_b (in the positive x-direction) and vertical displacement v_b (in the positive z-direction). In the linear analysis, there is no coupling between the horizontal and the vertical motion of the mass, which implies

$$\begin{aligned} u_b &= \Delta + (\varphi + \psi^{rel})H \\ v_b &= V \end{aligned} \tag{1}$$

By u_b^{rel} we will refer to the relative horizontal response $u_b^{rel} = \psi^{rel}H$. For a harmonic excitation, with circular frequency ω and time dependence $e^{-i\omega t}$, the system will respond with motion of the same frequency, i.e.

$$\psi^{rel} = \psi_0^{rel} e^{-i\omega t}$$

$$\mathbf{\Delta} = \mathbf{\Delta}_0 e^{-i\omega t}$$

where $\mathbf{\Delta} = \{V, \Delta, \varphi H\}^T$ is a generalized displacement vector, and $\mathbf{\Delta}_0 = \{V_0, \Delta_0, \varphi_0 H\}^T$ is the complex amplitude of $\mathbf{\Delta}$.

Motion of the building

From the free-body diagram of the oscillator (Figure 1), neglecting the moment of the vertical acceleration $-\omega^2 V_0 e^{-i\omega t}$, the equilibrium of moments about the centre of the base, O, implies

$$m_b \ddot{u}_b H + m_b r_b^2(\ddot{\varphi} + \ddot{\psi}^{rel}) + K_b \psi^{rel} + C_b \dot{\psi}^{rel} - m_b g(\varphi + \psi^{rel})H = 0 \tag{2}$$

where g is the acceleration due to gravity. On the left-hand side of equation (2), the first term is the moment about point O of the inertia forces due to translation of the oscillator mass, the second term is the moment of the inertia forces due to rotation of the oscillator mass about the point $\xi = 0$, the third and the fourth terms represent the moments of the elastic and of the damping forces, and the last term is the moment of the gravity forces. Equation (2) is equivalent to

$$\begin{aligned} &\ddot{\psi}^{rel} + 2\omega_N \zeta \dot{\psi}^{rel} + \omega_N^2 \psi^{rel} - \frac{m_b H^2}{I_0} \frac{g}{\omega_N^2 a} \frac{a}{H} \omega_N^2 \psi^{rel} \\ &\quad = \frac{-m_b H^2}{I_0} \frac{\ddot{\Delta}}{H} - \ddot{\varphi} + \frac{m_b H^2}{I_0} \frac{g}{\omega_N^2 a} \frac{a}{H} \omega_N^2 \varphi \end{aligned} \tag{3}$$

where $K_b/I_0 = \omega_N^2$ and $C_b/I_0 = 2\omega_N \zeta$. $I_0 = m_b H^2[1 + (r_b/H)^2]$ is the mass moment of inertia of the building about $\xi = 0$, and ω_N and ζ are the fixed-base natural frequency and the ratio of critical damping. The term $g/\omega_N^2 a$ is a dimensionless parameter involving the acceleration due to gravity. For low buildings this ratio is very small ($\sim 10^{-4}$), while for higher buildings it is of order 10^{-1}. For example, for a sixty storey

building with base $2a = 30$ m, it has a value $\sim 0{\cdot}3$. The damping raio, ζ, for typical buildings ranges between 0 and about 0·1. In calculating H and r_b for a two-dimensional equivalent SDOF oscillator that corresponds to a particular building, it is convenient first to model the building by a homogeneous shear beam[10] with height H_{sb} and width W_{sb} equal to the height and the smaller width of the building, and with mass per unit volume equal to the mass per unit volume for the building. Then, assuming that the equivalent SDOF oscillator has the same mass per unit length (in the y-direction) as the shear wall, H and r_b are related to H_{sb} and W_{sb} as follows: $H = H_{sb}/\sqrt{3}$ and $r_b = W_{sb}/\sqrt{12}$. For a very tall building, for example $H_{sb} = 250$ m, $r_b/H \approx 0{\cdot}08$ and for a short building $r_b/H \approx 0{\cdot}5$.

For a harmonic motion of the foundation, $\mathbf{\Delta} = \mathbf{\Delta}_0 e^{-i\omega t}$, from equation (3), the relative rocking angle ψ^{rel} can be expressed as a function of the displacement of the foundation as

$$\psi_0^{rel} = \frac{\dfrac{m_b H^2}{I_0}\left(\dfrac{\omega}{\omega_N}\right)^2 \dfrac{\Delta_0}{H} + \left[\left(\dfrac{\omega}{\omega_N}\right)^2 + \dfrac{g}{\omega_N^2 H}\dfrac{m_b H^2}{I_0}\right]\varphi_0}{1 - 2i\zeta\dfrac{\omega}{\omega_N} - \left(\dfrac{\omega}{\omega_N}\right)^2 - \dfrac{g}{\omega_N^2 H}\dfrac{m_b H^2}{I_0}} \tag{4}$$

Then, the forces that the foundation exerts onto the building (the vertical force $f_z^{(b)}$, the horizontal force $f_x^{(b)}$ and the moment about O, $M_0^{(b)}$) can be calculated in terms of the displacement of the foundation, from the dynamic equilibrium equations of the structure. $f_x^{(b)}$ is positive in the negative x-direction, $f_z^{(b)}$ is positive up and $M_0^{(b)}$ is positive counter-clockwise. Let $\mathbf{F}^{(b)} = \{f_z^{(b)}, f_x^{(b)}, M_0^{(b)}/H\}^T$ be a generalized force vector. Then, in matrix form one can write

$$\mathbf{F}^{(b)} = m_b \omega^2 [[K^{(b)}] + [C_g^{(b)}]]\mathbf{\Delta}_0 e^{-i\omega t} \tag{5}$$

where

$$[K^{(b)}] = \begin{bmatrix} k_{11} & 0 & 0 \\ 0 & k_{22} & k_{23} \\ 0 & k_{32} & k_{33} \end{bmatrix} \tag{6}$$

with

$$k_{11} = 1 \tag{7a}$$

$$k_{22} = 1 + \frac{m_b H^2}{I_0}\left(\frac{\omega}{\omega_N}\right)^2 \frac{1}{p} \tag{7b}$$

$$k_{23} = 1 + \left(\frac{\omega}{\omega_N}\right)^2 \frac{1}{p} \tag{7c}$$

$$k_{32} = k_{23} \tag{7d}$$

$$k_{33} = \frac{I_0}{m_b H^2}\left[1 + \left(\frac{\omega}{\omega_N}\right)^2 \frac{1}{p}\right] \tag{7e}$$

$$p = 1 - 2i\zeta\frac{\omega}{\omega_N} - \left(\frac{\omega}{\omega_N}\right)^2 - \frac{g}{\omega^2 H}\left(\frac{\omega}{\omega_N}\right)^2 \frac{m_b H^2}{I_0} \tag{7f}$$

is the complex stiffness matrix for the building, and

$$[C_g^{(b)}] = \frac{g}{\omega^2 H}\begin{bmatrix} 0 & 0 & 0 \\ 0 & 0 & c_{23} \\ 0 & c_{23} & c_{33} \end{bmatrix} \tag{8}$$

with

$$c_{23} = \frac{m_b H^2}{I_0}\left(\frac{\omega}{\omega_N}\right)^2 \frac{1}{p} \tag{9a}$$

$$c_{32} = c_{23} \tag{9b}$$

$$c_{33} = 1 + 2\left(\frac{\omega}{\omega_N}\right)^2 \frac{1}{p} + \frac{m_b H^2}{I_0}\left(\frac{\omega}{\omega_N}\right)^2 \frac{1}{p}\frac{g}{\omega^2 H} \tag{9c}$$

is the impedance matrix associated with the gravity forces acting on the building.

Equilibrium of the foundation

Figure 2 shows the free-body diagram of the foundation where $f_x^{(b)}, f_z^{(b)}$ and $M_0^{(b)}$ are the horizontal and vertical forces and the moment that the building exerts onto the foundation; $f_x^{(s)}, f_z^{(s)}$ and $M_0^{(s)}$ are the horizontal and vertical forces and the moment applied onto the foundation by the elastic half-space; $m_f \ddot{\Delta}$, $m_f \ddot{V}$ and $I_0^{(f)} \ddot{\varphi}$ are the D'Alambert forces of the foundation; and $m_f g$ and point C are its gravity force and centre of gravity, respectively. All of these forces act at point O on the foundation. $I_0^{(f)}$ is the mass moment of inertia of the foundation about point O. Let $\mathbf{F}^{(s)} = \{f_z^{(s)}, f_x^{(s)}, M_0^{(s)}/H\}^T$ be a generalized force vector. $\mathbf{F}^{(s)} = \mathbf{F}_0^{(s)} + \mathbf{F}_\Delta^{(s)}$, where $\mathbf{F}_0^{(s)}$ and $\mathbf{F}_\Delta^{(s)}$ are generalized force vectors representing the foundation driving forces (forces acting on the foundation at rest, and due to the free-field motion) and the forces induced in the half-space due to the deformations caused by the moving foundation, in the absence of incident waves. $\mathbf{F}_0^{(s)}$ is equal in magnitude and of opposite direction to the force that must be applied to the foundation to keep it at rest, while it is forced to move by the free-field incident waves. Consequently, $\mathbf{F}_0^{(s)}$ depends[10] only on the characteristics of the free-field motion (type of incident waves, angle of incidence and their amplitude), $\mathbf{F}_\Delta^{(s)}$ depends on the imposed motion $\boldsymbol{\Delta}$, and they both depend on the shape of the foundation and on the frequency of the excitation. $\mathbf{F}_\Delta^{(s)}$ can be written as

$$\mathbf{F}_\Delta^{(s)} = -2\mu[Q]\boldsymbol{\Delta} \tag{10}$$

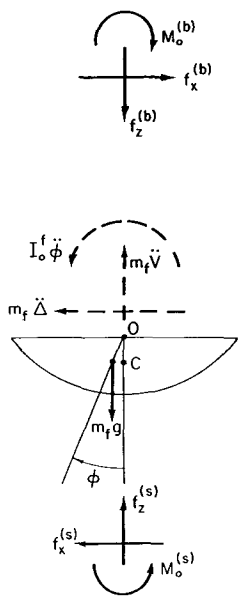

Figure 2. Equilibrium of forces acting on the foundation at point O

where $2\mu[Q]$ is the impedance matrix for the foundation and μ is the shear modulus of the half-space.[10]

The equilibrium equations of the foundation are

$$[M_f]\ddot{\Delta} = \mathbf{F}^{(b)} - \mathbf{F}^{(s)} - \mathbf{F}_g^{(f)} \tag{11}$$

where $[M_f] = \text{diag}\{m_f, m_f, I_0^{(f)}/H^2\}$ is the mass matrix of the foundation, and $\mathbf{F}_g^{(f)} = \{0, 0, m_f gc\varphi\}^T$ is the generalized force vector of the gravity forces of the foundation (c is the depth to the centre of gravity). Then, for given characteristics of the structure and for various types of excitations, equation (11) can be solved for Δ.

RESULTS AND ANALYSIS

System parameters

Definition of the dimensionless parameters. Since the intensity of scattering of the waves from the building foundation and the interaction between the building motion and the soil depend on the size of the foundation relative to the wavelength of the incident waves, and on the stiffness of the building, compared with the stiffness of the soil, the dimensionless quantities $\eta = 2a/\beta T = \omega a/\pi\beta$ and $\eta_N = 2a/\beta T_N = \omega_N a/\pi\beta$, respectively, will be used in the analysis, rather than the frequencies ω and ω_N. The meaning of η is the number of wavelengths of the S-waves in the soil, with frequency ω, contained in length equal to the width of the foundation. Then η_N is the value of η when the frequency of the S-waves is equal to the natural frequency of the building, ω_N. Other dimensionless parameters that affect the response of the building–foundation–soil system are the mass ratios m_b/m_f and m_f/m_s, where m_s is the mass per unit length in the y-direction of the soil replaced by the foundation. The ratios m_b/m_f and m_f/m_s are related to the ratios of the corresponding material densities with the help of a shear beam building model. For example, $m_b = \rho_b W_{sb} H_{sb}$ 1 and $m_f = \rho_f A_f$ 1, where A_f is the cross-sectional area of the foundation. Typically, the ratio of the mass density of the building and of the soil is $\rho_b/\rho_s = 0{\cdot}2$.[5] We assume in our calculations that the foundation density is also 0·2 times the density of the soil. This implies that, typically, $m_f/m_s = 0{\cdot}2$ and $m_b/m_f \approx 2{\cdot}2\,H/a$ for a semi-circular foundation. In all of the presented results $m_f/m_s = 0{\cdot}2$. The building mass takes values approximately equal to the typical value, or values that are approximately two times larger or half of the typical value. Typically, η_N ranges in the interval 0–0·6, and H/a between 0·5 and 3. In the presented numerical results, $0 < \eta_N \leqslant 0{\cdot}3$, $H/a = 2$ and 5, and the building damping ratio $0 \leqslant \zeta \leqslant 0{\cdot}12$. $\zeta = 0{\cdot}12$ is a high value for the damping in the building, and it was used only to help recognize more easily the trends of the system damping and of the base rocking with changing ζ.

For example, for a 10 storey building (natural frequency $f_N = 1$ Hz and base half-width $a = 15$ m), situated on good soil with shear wave velocity $\beta = 400$ m/s, for the lumped mass model $H/a \approx 1{\cdot}9$ and $\eta_N \approx 0{\cdot}076$. On the other hand, for a nuclear power plant containment structure[5] (natural frequency $f_N = 5$ Hz and $a = 23$ m), situated on harder soil ($\beta = 800$ m/s), $\eta_N \approx 0{\cdot}28$. The same 10 storey building in Los Angeles ($\beta \approx 250$ m/s) would have $\eta_N \approx 0{\cdot}12$, and in Mexico City, where the shear wave velocity in the soil can be as low as 40–100 m/s, $\eta_N \approx 0{\cdot}3$–$0{\cdot}75$.

η_N depends on the ratio of the stiffness of the building and of the half-space, and on the ratio of the mass of the building and the mass of the soil replaced by the foundation. For a semi-circular foundation

$$\eta_N = \frac{\omega_N a}{\pi\beta} = \sqrt{\frac{K_b}{\mu a}}\sqrt{\frac{m_s}{m_b}}\sqrt{\frac{2}{\pi^3}}\frac{1}{\sqrt{1+\left(\frac{r_b}{H}\right)^2}}\frac{a}{H}$$

Small η_N means a flexible building and/or stiff soil and large η_N means a stiff building and/or very flexible soil. The limiting value $\eta_N \to 0$ corresponds to the case of a flexible building on a rigid half-space excited by horizontal motion at the base $\Delta e^{-i\omega t}$ (fixed-base building model, no interaction). $\eta_N \to \infty$ corresponds to a rigid building oscillating together with the foundation as a single rigid body.

Input excitation. We consider incident plane SV-waves, with incident angles $\gamma = 0°$, 20°, 30° ($= \gamma_{crit}$), 45°, 60° and 85°, where γ_{crit} is the critical angle,[10] and incident plane P-waves with incident angles $\gamma = 0°$, 30°, 60°

and 85°. (γ is the angle between the direction of propagation of the incident wave and the normal to the half-space surface.) The Poisson's ratio $\nu = 0{\cdot}3333$. The effect of the gravity forces is neglected.

Definition of system frequency and system damping. By 'system frequency', and by 'system damping', we will refer to the frequency, and to the usual measure of the width of the peak, of the amplitude of the transfer function between the relative building response, u_b^{rel}, and the incident wave. The system frequency will be expressed in terms of the dimensionless frequency η and will be denoted by η_{sys}, and the system damping ratio will be denoted by ζ^{sys}.

We will measure ζ^{sys} from the amplitude spectrum of the relative building response, using the analogy with the half-power method for a SDOF oscillator. Therefore, we will measure the frequency of the peak of the response, η^{sys}, and the frequencies to the left and to the right of η^{sys} (η_1 and η_2) for which $u_b^{rel} = u_b^{rel}(\eta^{sys})/\sqrt{2}$. Then ζ^{sys} can be calculated as

$$\zeta^{sys} = \frac{\eta_2 - \eta_1}{\eta_1 + \eta_2} \approx \frac{\eta_2 - \eta_1}{2\eta^{sys}}$$

The relative building response is calculated using the equations in the previous section, and solving the system of equations (11) for Δ. No additional approximations and assumptions, are made. To reduce the calculation effort, the foundation driving force $\mathbf{F}_0^{(s)}(\eta)$ and the soil impedance matrix $[Q(\eta)]$ were calculated

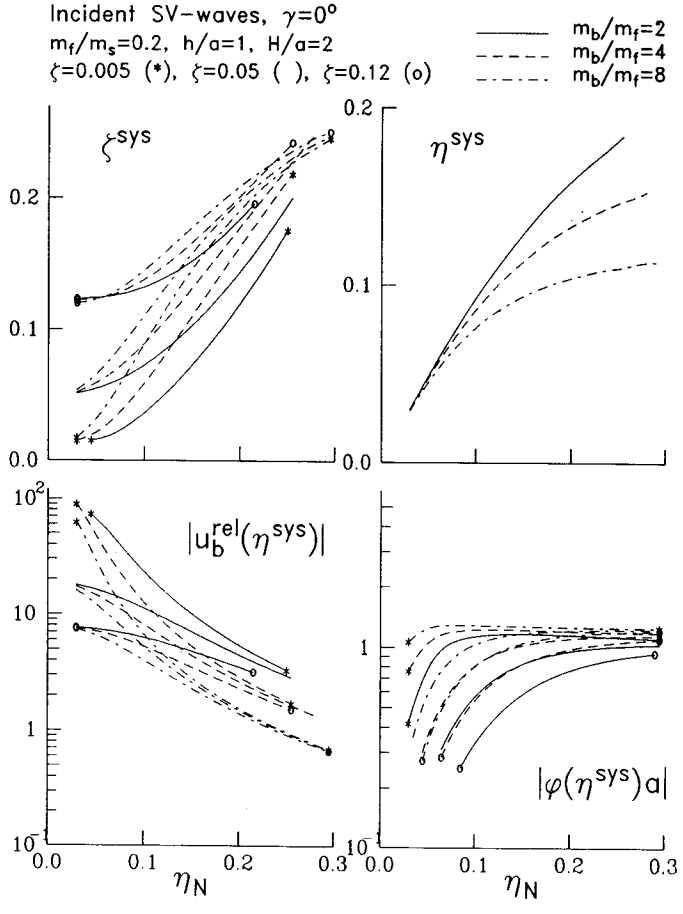

Figure 3. The system damping ratio, ζ^{sys}, the system frequency, η^{sys}, the peak relative building response, $|u_b^{rel}(\eta^{sys})|$, and the peak base rocking response, $|\varphi^{rel}(\eta^{sys})a|$, versus the relative stiffness parameter, η_N, for a medium high building ($H/a = 2$) on a semi-circular foundation

only once (at selected frequencies) for a given type of excitation and foundation shape. Their values were then substituted in equation (11) for different combinations of the remaining parameters. The damping was measured from the transfer function amplitude, calculated from equation (11) at frequencies equally spaced at $\Delta\eta = 0{\cdot}0017125$. Interpolation by cubic splines is used between these points, to determine the peak and the half-power points in the spectrum.

Vertically incident SV-waves and semi-circular foundation

For vertically incident SV-waves, the free-field motion (motion resulting from the interference of the incident wave and the wave reflected from the half-space surface in the absence of any inhomogeneities or irregularities) does not have a rotational component or a vertical component, on the ground surface. However, because of the embedment, the foundation input motion (response of a massless foundation in the absence of the superstructure) does have rotation[10] owing to the finite size of the embedment, relative to the wavelength of the incident waves, and because of the anti-symmetric nature of the displacement of the free-field motion, with respect to the vertical axis of symmetry of the foundation. So, in general the foundation will rotate because of the rotation of the foundation input motion and because of the action of the forces from the superstructure.

In Figure 3, the system damping, ζ^{sys}, the system frequency, η^{sys}, the amplitude of the peak relative building response, $|u_b^{rel}(\eta^{sys})|$, and the amplitude of the peak base rotation, $|\varphi(\eta^{sys})a|$, have been plotted versus the

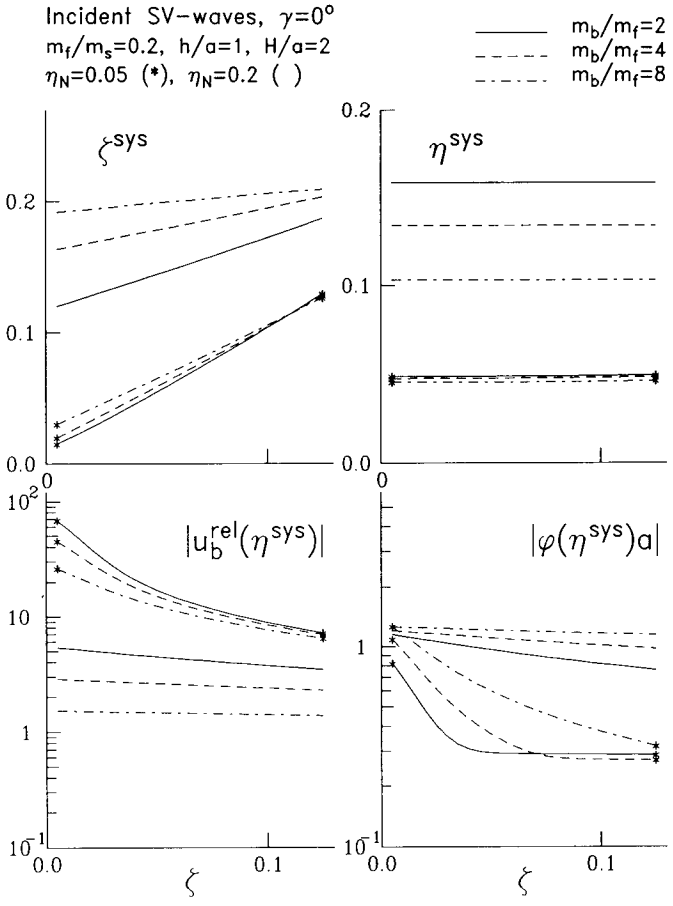

Figure 4. The system damping ratio, ζ^{sys}, the system frequency, η^{sys}, the peak relative building response, $|u_b^{rel}(\eta^{sys})|$, and the peak base rocking response, $|\varphi^{rel}(\eta^{sys})a|$, versus the damping ratio in the building, ζ, for a medium high building ($H/a = 2$) on a semi-circular foundation

'relative stiffness' parameter η_N for a typical building ($H/a = 2$), with damping ratios $\zeta = 0{\cdot}005$, $0{\cdot}05$ and $0{\cdot}12$, and mass ratios $m_b/m_f = 2$, 4 and 8 ($m_b/m_f = 4$ corresponds to the typical value of ρ_b/ρ_s). In Figure 4, the same quantities are shown as functions of ζ, for a building with the same values of H/a and m_b/m_f, and for $\eta_N = 0{\cdot}05$ and $0{\cdot}2$. In Figures 5 and 6 the same functional relationships are shown as in Figures 3 and 4, but for a higher building, with $H/a = 5$, and with $m_b/m_f = 5$, 10 and 20 ($m_b/m_f = 10$ corresponds to the typical value of ρ_b/ρ_s). Since the system frequency does not depend on the damping in the building, in Figures 3 and 5, η^{sys} is shown only for $\zeta = 0{\cdot}05$.

Asymptotic behaviour as $\eta_N \to 0$ *and as* $\eta_N \to \infty$. When the soil is stiffer, the system response is influenced more by the damping in the building, while, when it is more flexible, it is affected more by the building mass and height. This can be concluded from Figures 3 and 5, where, as $\eta_N \to 0$, the curves corresponding to the same value of ζ merge together, while, as $\eta_N \to \infty$, the curves with same value of m_b/m_f merge together. As $\eta_N \to 0$ the system response approaches the response of a fixed-base building model; then $\eta^{sys} \to \eta_N$, $\zeta^{sys} \to \zeta$, $u_b^{rel}(\eta^{sys}) \to u_b^{rel}(\eta_N)$ and $\varphi \to 0$; the dissipation of the building energy through radiation into the soil then becomes smaller and goes to 0 in the limit.

As $\eta_N \to \infty$, the system response approaches the response of a rigid building oscillating in the semi-infinite elastic soil medium; then $\zeta^{sys}(\eta_N)$, $\eta^{sys}(\eta_N)$ and $\varphi(\eta_N)$ have horizontal asymptotes that depend on the building mass and height, and $u_b^{rel} \to 0$. Then $\eta^{sys} \to \eta^{rig}$, the system frequency of a rigid building, which is lower when the building is 'heavier'; $|\varphi(\eta^{sys})| \to \varphi^{rig}$, the base rocking when the building is rigid, which is larger when the

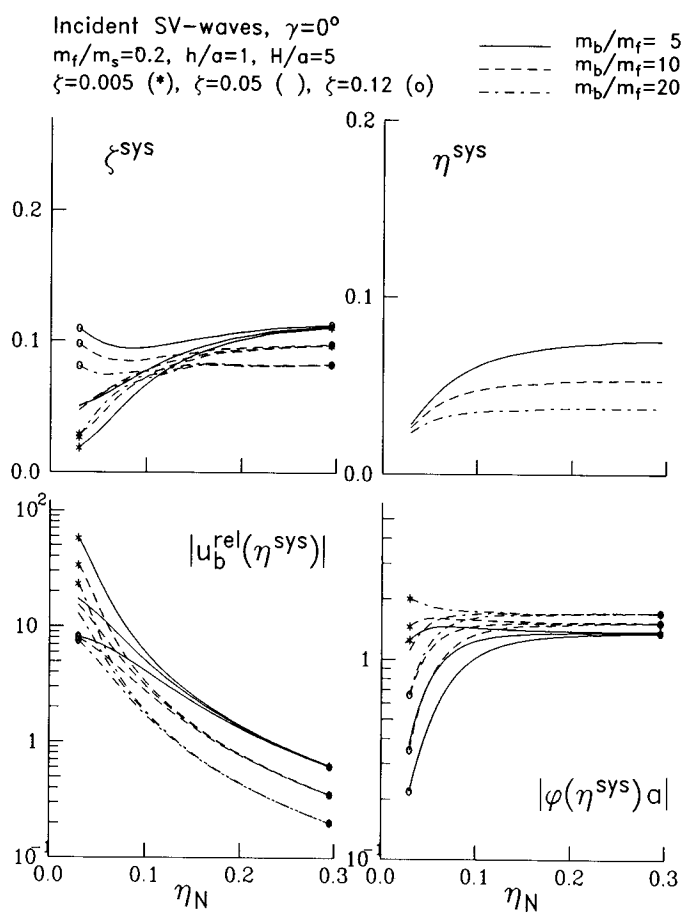

Figure 5. The system damping ratio, ζ^{sys}, the system frequency, η^{sys}, the peak relative building response, $|u_b^{rel}(\eta^{sys})|$, and the peak base rocking response, $|\varphi^{rel}(\eta^{sys})a|$, versus the relative stiffness parameter, η_N, for a higher building ($H/a = 5$) on a semi-circular foundation

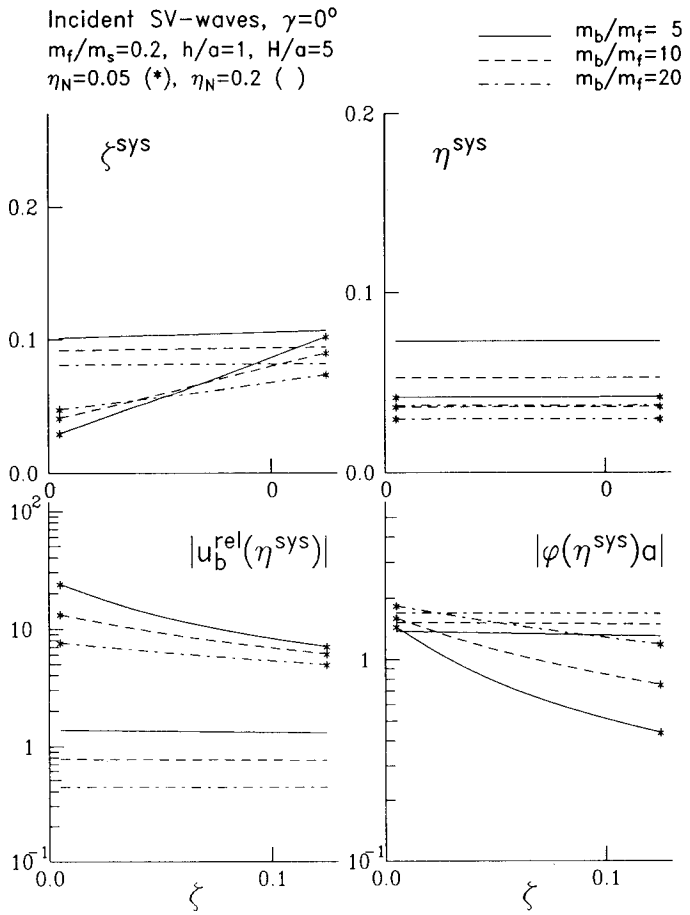

Figure 6. The system damping ratio, ζ^{sys}, the system frequency, η^{sys}, the peak relative building response, $|u_b^{rel}(\eta^{sys})|$, and the peak base rocking response, $|\varphi^{rel}(\eta^{sys})a|$, versus the damping ratio in the building, ζ, for a higher building ($H/a = 5$) on a semi-circular foundation

building mass is larger;[10] $\zeta^{sys} \to \zeta^{rig}$, the system frequency of the motion of the base of a rigid building, relative to the free-field motion, which is smaller when the building mass is larger. (The peak of the transfer function of the motion of the rigid building, relative to the free-field motion, is sharper and higher when the building is higher and heavier.)

System behaviour for intermediate η_N. The results show that, for intermediate values of η_N, when both the building and the soil are flexible, for a given shape of the foundation[11] and building height, the peak relative building response is smaller, the peak base rocking response is larger and the system frequency is lower when the building mass is larger (Figures 3 and 5). When the soil is stiffer (lower η_N), the system damping ratio is larger for 'heavier' buildings. However, for sufficiently large η_N, when the system behaves more like a rigid body, the system damping ratio is smaller when the building is 'heavier'.

It can be seen from the results in Figures 3 and 5 that the peak relative response $|u_b^{rel}(\eta^{sys})|$ is always smaller when the soil is 'softer' (when η_N is larger). However, this may not always be the case when there is damping in the soil.[2,5] The system damping ratio may increase or decrease with η_N depending on how large ζ in the building is compared with ζ^{rig}, the limit of ζ^{sys} when $\eta_N \to \infty$. In most of the cases that we considered, $\zeta < \zeta^{rig}$ and ζ^{sys} monotonically increases with increasing η_N. However, in the extreme case of very high structural damping (e.g. $\zeta = 0{\cdot}12$) and a high building ($H/a = 5$), $\zeta > \zeta^{rig}$. Then, as the soil becomes more flexible (η_N increases), and the contribution of the building damping to the system damping ratio becomes smaller, the

system damping decreases, and, as the example shows, it can be smaller than the damping in the building. It can be seen from Figure 5 that even when this happens, the peak relative response is still smaller than the fixed-base response. So, $\zeta^{sys} < \zeta$ does not imply that the relative building response is larger than the response calculated when the soil–structure interaction effects are not included (the fixed-base response). However, this may not be true for a MDOF equivalent oscillator and when the soil has material damping.

It can be seen from Figures 3 and 5 that, in the lower range of η_N, the base rocking is larger when the soil is more flexible. It is larger when the building damping is smaller. For sufficiently high η_N, when the building behaves more like a rigid body, as η_N increases, $|\varphi(\eta^{sys})|$ approaches monotonically the limit, which is the rocking response of a rigid building. It may monotonically increase or decrease while approaching this limit depending on how large it had grown in the region of lower values of η_N.

System response versus ζ. From the curves in Figures 4 and 6, the following can be seen. The system frequency η^{sys} does not depend on ζ. The relative building response decreases with ζ at a higher rate when the building is lower, lighter and on harder soil and it practically does not depend on ζ when the building is sufficiently high, heavy and on sufficiently soft soil.

All the curves $\zeta^{sys}(\zeta)$ are practically straight lines with the slope having values between 1 and 0 and a value at $\zeta = 0$ depending on m_b/m_f, H/a and η_N. Because there is no damping in the soil, when $\zeta = 0$ the system damping is due only to radiation and scattering. For the lower and lighter building ($H/a = 2$ and $m_b/m_f = 2$, 4 and 8, Figure 4), when the building is sitting on harder soil ($\eta_N = 0{\cdot}05$), the slope of $\zeta^{sys}(\zeta)$ is close to 1 and $\zeta^{sys}(\zeta = 0)$ is small. For heavier buildings (Figure 4) and on softer soil ($\eta_N = 0{\cdot}2$), the slope of $\zeta^{sys}(\zeta)$ is small (the rate of change of ζ^{sys} with ζ is small) and $\zeta^{sys}(\zeta = 0)$ is larger. ζ^{sys} practically does not depend on ζ when $H/a = 5$ and $m_b/m_f = 5$, 10 and 20 (Figure 6). It can be concluded that, for a tall and heavy building, the system damping practically does not depend on the damping in the building.

When the building is lower, and when it is on harder soil ($H/a = 2$, $\eta_N = 0{\cdot}005$), the system damping ratio is larger when the building mass is larger. For the higher building and on softer soil ($H/a = 5$ and $\eta_N = 0{\cdot}2$, Figure 6), for all values of ζ the system damping ratio is smaller when the building mass is larger (the system behaves as a rigid body). From the values of ζ at which the curves for different values of m_b/m_f cross each other, it can be concluded that it also depends on the value of the building damping whether the system will behave more like a rigid body or like a flexible structure. For $H/a = 2$ and $\eta_N = 0{\cdot}05$ (Figure 4), the curves $\zeta^{sys}(\zeta)$ cross each other at $\zeta \approx 0{\cdot}11$, and for $H/a = 5$ and $\eta_N = 0{\cdot}05$ (Figure 6) at $\zeta \approx 0{\cdot}05$–$0{\cdot}06$. From this, it can be concluded that buildings with larger damping act 'stiffer'.

If the line $\zeta^{sys} = \zeta$ is drawn, it can be seen that, in Figure 4 ($H/a = 2$), ζ^{sys} is greater than the damping in the building. For the higher building (Figure 6), however, for sufficiently large ζ the system damping ratio is lower than the damping ratio in the building.

From the curves $\varphi(\zeta^{sys})$ in Figures 4 and 6 it can be seen that, for system configurations for which the structural damping affects the system response, the rocking of the base is smaller when the damping in the building is larger.

Reduction of the system frequency, η^{sys}/η_N. The reduction of the system frequency, relative to the fixed-base frequency, is illustrated in Figure 7, where the ratio η^{sys}/η_N has been plotted versus η_N for buildings of different heights and masses ($H/a = 2$, $m_b/m_f = 2$, 4 and 8; $H/a = 5$, $m_b/m_f = 5$, 10 and 20; and $H/a = 10$, $m_b/m_f = 10$, 20 and 40). It can be seen that the reduction is larger when H/a is larger and, for buildings with the same height, when m_b/m_f is larger. For example, for the 10-storey building ($H/a \approx 2$, and $m_b/m_f = 4$), when the shear wave velocity in the soil $\beta = 400$ m/s, $\eta^{sys}/\eta_N \approx 92$ per cent; when $\beta = 250$ m/s (e.g. Los Angeles basin), $\eta^{sys}/\eta_N \approx 75$ per cent; and when $\beta = 50$ m/s (e.g. Mexico City valley), $\eta^{sys}/\eta_N \approx 55$ per cent.

Effects of the type of incident waves and of the incident angle

Because of the scattering and diffraction of the incident waves from the foundation, and because of the filtering effect of the foundation for shorter wavelengths of the incident waves, the foundation input motion differs from the free-field motion. (Foundation input motion is the response of a massless foundation under the action of the incident waves and in the absence of the building.) The free-field motion on the half-space

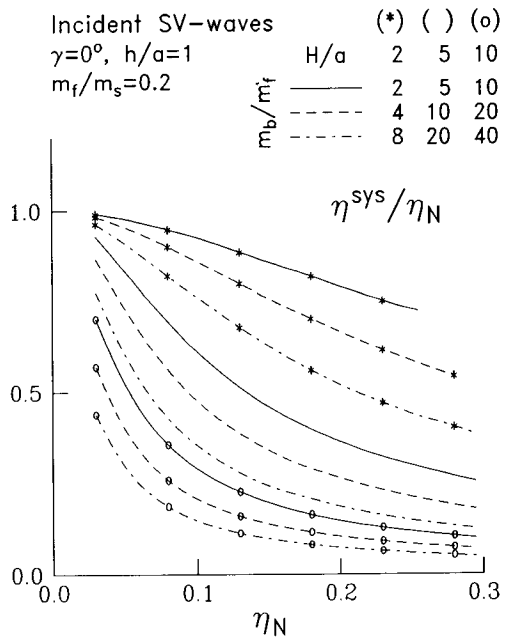

Figure 7. Reduction of the system frequency relative to the fixed-base frequency, η^{sys}/η_N, for several buildings on semi-circular foundations

surface, and, therefore, the foundation input motion amplitudes and phases, depend significantly on the type of incident waves and their angle of incidence.[10,12] The horizontal component and the point rotation of the free-field motion may differ considerably in amplitude, depending on the incident angle and the type of incident waves. However, in practice, the wave nature of the earthquake excitation of buildings is usually ignored. The actual excitation, which consists of translations and rotations, is approximated by a synchronous horizontal motion of the base, which corresponds to vertically incident, long compared with the foundation size, plane SV-waves.

To see the effect of the type of incident waves and their angle of incidence on the system damping ratio and on the relative building response, in Figures 8 and 9, ζ^{sys} and $|u_b^{rel}|$, normalized by the horizontal free-field amplitude on the half-space surface, $|u^{ff}|$, have been plotted versus η_N for buildings with $H/a = 2$, $m_b/m_f = 2$, 4 and 8, and for $\zeta = 0{\cdot}05$. In Figure 8, the excitation is an SV-wave with incident angles $\gamma = 0°$, 20°, 30°, 45°, 60° and 85°; in Figure 9, it is an incident P-wave with $\gamma = 30°$, 60° and 85°, and a vertically incident SV-wave (drawn in both figures as reference). The critical angle, γ_{crit}, for the incident plane SV-waves is 30°. Our results show that the system frequency practically does not depend on the type of incident waves and on the incident angle. It can be seen that, for incident P-waves and SV-waves with $\gamma \leqslant \gamma_{crit}$, ζ^{sys} takes very similar values. The ratios $|u_b^{rel}|/|u^{ff}|$ are also practically the same. However, for incident SV-waves with incident angles $\gamma > \gamma_{crit}$, the difference in ζ^{sys} for larger values of η_N is noticeable. The differences in the $|u_b^{rel}|/|u^{ff}|$ ratios can also be significant even for smaller η_N, as can be seen from Figure 8. For $\gamma = 45°$ $|u_b^{rel}|/|u^{ff}|$ tends to infinity for all η_N's and therefore has not been plotted. It can be seen from these figures that the difference in ζ^{sys} increases with increasing η_N (increasing flexibility of the soil). Similar behaviour is observed for the higher buildings.[11]

The reason for the dependence of ζ^{sys} and $|u_b^{rel}|/|u^{ff}|$ on the type of incident waves and incident angle comes from the differences in the components of the foundation input motion.[10] What makes the case of incident SV-waves with $\gamma > \gamma_{crit}$ different from the rest of the considered excitations is the presence of a considerable amount of rotation in the foundation input motion, as compared with the horizontal translation, due to the inhomogeneous wave in the free-field motion. The input base rocking represents an additional excitation to the base input translation, and it is responsible for the higher values of the ratio $|u_b^{rel}|/|u^{ff}|$. When $\gamma = 45°$ it is the only excitation, since, then, the input base translation is equal to zero.[10,12] It also changes the shape of the system transfer function (causes larger relative response away from the system frequency) and, therefore,

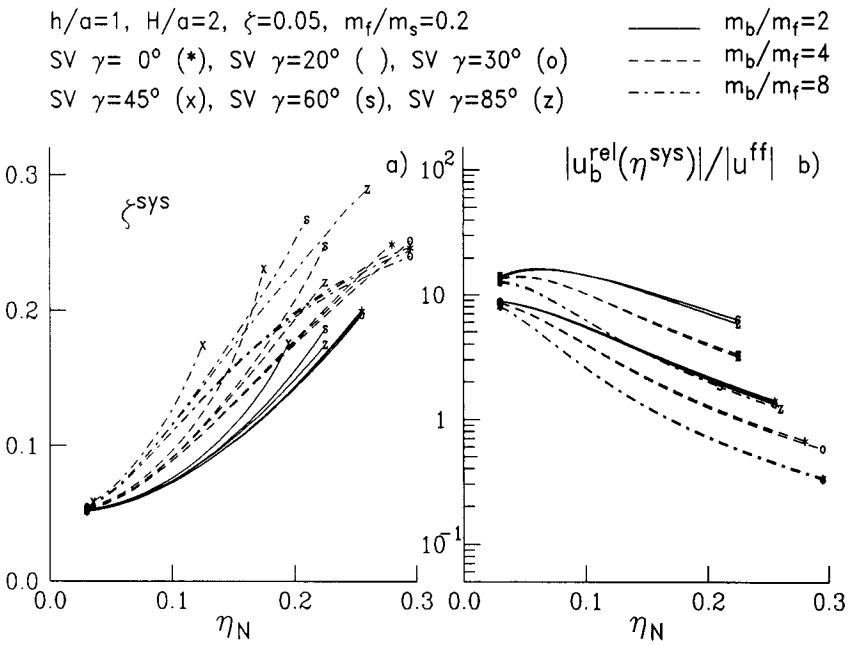

Figure 8. The system damping ratio, ζ^{sys}, and the peak relative building response, $|u_b^{rel}(\eta^{sys})|$, normalized with the horizontal free-field surface displacement, $|u^{ff})|$, for incident plane SV-waves with incident angles $\gamma = 0°, 20°, 30°, 45°, 60°$ and $85°$ and for building damping ratio $\zeta = 0.05$

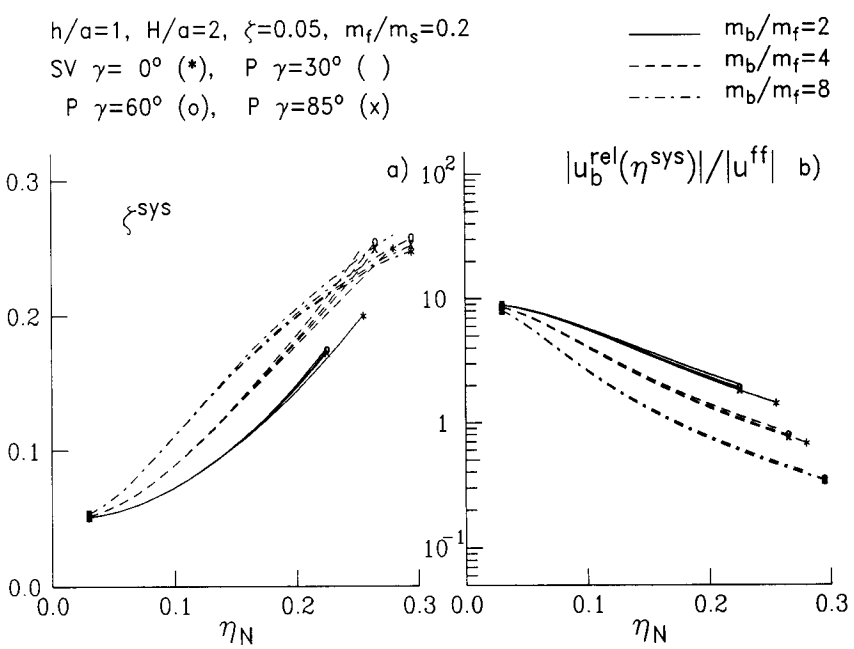

Figure 9. The system damping ratio, ζ^{sys}, and the peak relative building response, $|u_b^{rel}(\eta^{sys})|$, normalized with the horizontal free-field surface displacement, $|u^{ff})|$, for incident plane P-waves with incident angles $\gamma = 30°, 60°$ and $85°$ and for building damping ratio $\zeta = 0.05$

affects the system damping. It affects the phases of the base horizontal and rocking response, relative to the phase of the building relative response. The base rocking is, then, a vector sum of the input rocking and the rocking due to the inertia forces of the building. From our definition of the system damping, larger ζ^{sys} simply means wider peaks of $|u_b^{rel}|$ and of $|\varphi|$, since η^{sys} does not depend on the type of excitation.

To illustrate the extent and the effect of this 'additional' excitation, in Figure 10 the transfer function amplitudes and phases of Δ, φ and u_b^{rel} have been plotted for incident SV-waves with $\gamma = 30°$ and $60°$. The model is a higher building ($H/a = 2$, $m_b/m_f = 4$), with low damping ($\zeta = 0{\cdot}005$) and situated on softer soil ($\eta_N = 0{\cdot}2$). The system frequency is $\eta^{sys} = 0{\cdot}13$. At the system frequency, and for these incident angles, the amplitudes of the input base translation are $\Delta^{inp} = 2{\cdot}9$ and $1{\cdot}97$, and of the input base rotations are $\varphi^{inp}H = 0{\cdot}3$ and $1{\cdot}38$. The ratio $|\varphi^{inp}H|/|\Delta^{inp}| = 0{\cdot}1$ and $3{\cdot}9$. The relative responses are $|u_b^{rel}| = 4{\cdot}6$ and 2. It can be seen that the rotation amplitude $|\varphi|$ for $\gamma = 60°$ does not have a maximum at $\eta = \eta^{sys}$, but at a lower η, similar to $|\Delta|$. The shapes of the phases of Δ and φ are practically reversed fo $\gamma = 30°$ and for $\gamma = 60°$. The quantity $\Delta^{inp} + \varphi^{inp}H$ would thus seem more representative for the building excitation than Δ^{inp} alone.

To illustrate how different the system response would be if the wave passage effects (kinematic interaction) are not included, in Figure 11, ζ^{sys}, η^{sys}, $|u_b^{rel}(\eta^{sys})|/|u^{ff}|$ and $|\varphi(\eta^{sys})|/|u^{ff}|$ are plotted versus η_N when the foundation is driven only by a horizontal motion with amplitude $|\Delta| = 2$ (the solid lines). For comparison, the response to excitation by incident SV-waves with incident angles $\gamma = 0°, 20°, 30°, 45°, 60°$ and $85°$ (the dashed lines) is also shown. Different symbols are used to distinguish the lines for different incident angles. The building height is such that $H/a = 2$, the foundation is semi-circular ($h/a = 1$), the damping in the building is $\zeta = 0{\cdot}005$, and the mass ratios are $m_b/m_f = 4$ and $m_f/m_s = 0{\cdot}2$. Input horizontal displacement $\Delta = 2e^{-i\omega t}$ for the foundation corresponds to excitation by vertically incident plane SV-waves of infinitely long wavelength, compared to the size of the foundation. In this approximation of the foundation input motion, the scattering of the incident waves by the foundation and the filtering effect for shorter incident wavelengths are ignored. It

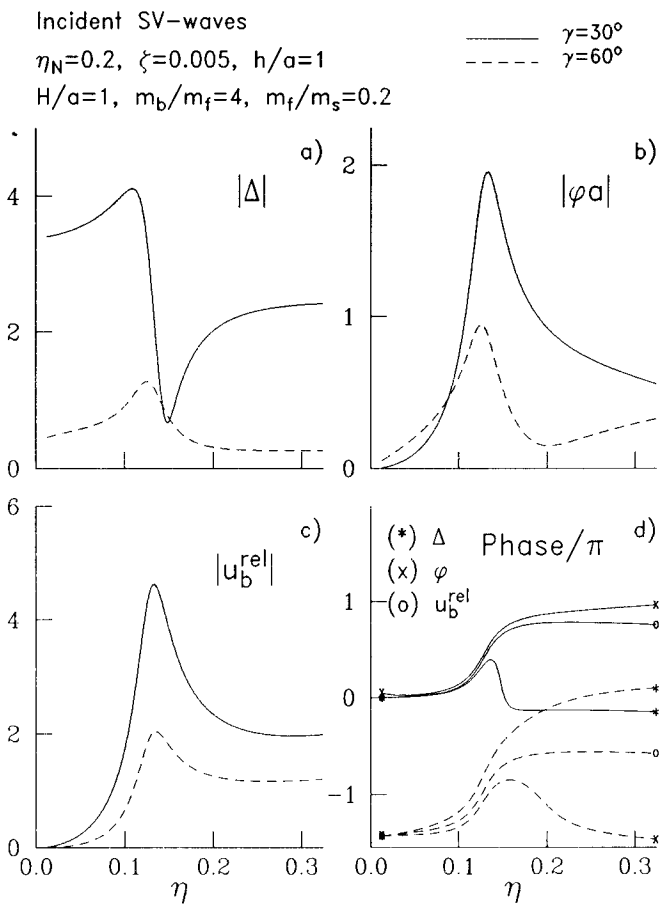

Figure 10. Transfer function amplitudes and phases of the base and of the building relative response for incident plane SV-waves with incident angles $\gamma = 30°$ and $60°$

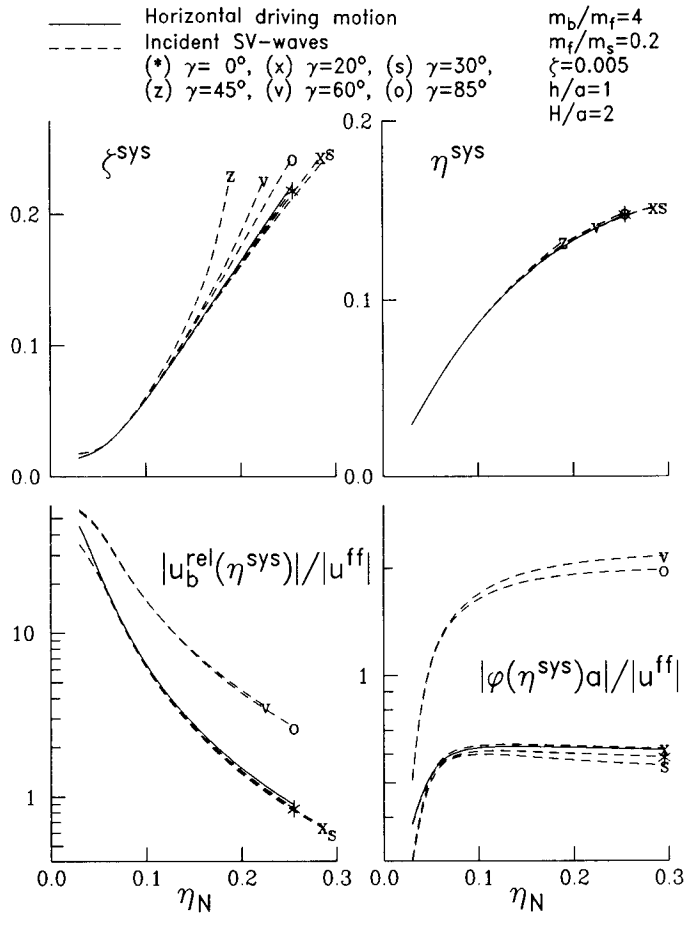

Figure 11. The system damping ratio, ζ^{sys}, the system frequency, η^{sys}, the normalized peak relative building response, $|u_b^{rel}\eta^{sys}|/|u^{ff}|$, and the normalized peak base rocking response, $|\varphi^{rel}(\eta^{sys})a|/|u^{ff}|$, versus the relative stiffness parameter, η_N, for incident plane SV-waves (the dashed lines), and for horizontal input driving motion with constant amplitude $|u^{ff}|$ (the solid lines)

can be seen from this figure that, when the wave passage effects are ignored, the system damping ratio is very close to the values for incident angles $\gamma \leqslant \gamma_{crit}$, but it is smaller than the values for $\gamma > \gamma_{crit}$ ($\gamma = 45°$, 60° and 85°). The building relative response, normalized by the amplitude of the driving displacement, Δ, also has very similar peak amplitudes to the ones corresponding to incidence below the critical angle, but significantly smaller than the peak amplitudes for incidence beyond the critical angle. $|u_b^{rel}(\eta^{sys})|/|u^{ff}|$ and $|\varphi(\eta^{sys})|/|u^{ff}|$ are not plotted for $\gamma = 45°$, because for this incident angle $|u^{ff}| = 0$. The peak rocking response, normalized by $|u^{ff}|$, also has similar amplitudes to the case for incidence below the critical angle, but noticeably smaller amplitudes than for incidence beyond the critical angle. This means that, for incident angles below the critical angle, most of the base rotation comes from the inertia forces of the building. It can be concluded that, if the wave passage effects are excluded from the analyses, by assuming simplified excitation, the system damping ratio, and the amplitudes of the system response, may be underestimated. These effects appear to be caused by the inhomogeneous part of the free-field motion, for incident angles greater than the critical angle. For incident plane P-waves, the same conclusions hold as for incident plane SV-waves below the critical angle.

Comparison with results by other authors

The earlier studies are for three-dimensional models, and, therefore, no direct comparison of our results with the results of these studies is possible. However, the trends of the system response with η_N and ζ are

similar. Functional relationships between the system parameters were developed by Bielak[2,4] and by Luco.[5] Our results for the system damping as a function of the relative stiffness parameter η_N are very similar to their analytical expressions. In terms of our dimensionless parameters, their equations for the system frequency and for the system damping are

$$\frac{1}{(\eta^{sys})^2} = \frac{1}{\eta_N^2} + \frac{1}{\eta_R^2} + \frac{1}{\eta_H^2} \tag{12}$$

where η_R and η_H are the rocking and the horizontal frequencies, in terms of the dimensionless frequency η, and

$$\zeta^{sys}(\eta^{sys}) = \left(\frac{\eta^{sys}}{\eta_N}\right)^3 \zeta + \left[1 - \left(\frac{\eta^{sys}}{\eta_N}\right)^2\right] \zeta_s + \left(\frac{\eta^{sys}}{\eta_H}\right)^3 \zeta_H + \left(\frac{\eta^{sys}}{\eta_R}\right)^3 \zeta_R \tag{13}$$

where ζ_s, ζ_H and ζ_R are the material soil, the horizontal and the rocking damping ratios. From equation (12) it follows that, as the soil flexibility increases (as $\eta_N \to \infty$), $\eta^{sys} \to \eta^{rig}$ which satisfies

$$\frac{1}{\eta^{rig^2}} = \frac{1}{\eta_R^2} + \frac{1}{\eta_H^2} \tag{14}$$

As the soil becomes very stiff (as $\eta_N \to 0$) $\eta^{sys} \to \eta_N$. The participation factors for the different damping ratios in the equation for ζ^{sys} depend on how close η^{sys} is to η_N or to η^{rig}. The contribution of ζ is the largest when the soil is very stiff, and it decreases as the soil becomes more flexible. The opposite holds for the participation factors of ζ_s, ζ_H and ζ_R. Analysis of the effects of the embedment depth and of the building mass on the system response as seen in 3D models (on prismatic foundations) and 2D models (on circular foundations) can be found in Reference 9.

The aim of the present study has been to help understand and explain the influence of the various system parameters on the system damping and on the system frequency, for a very simple two-dimensional model. However, the real world is more complicated than this model. The soil under the building is not a homogeneous half-space, it may be non-linear, it also has material damping, and the linear analysis holds only for small displacements. The conclusions and the results presented in this paper must be taken also with consideration that the model neglects the contribution of the higher modes to the building relative response and that the damping in the soil is ignored.

SUMMARY AND CONCLUSIONS

A two-dimensional analytical model has been employed to measure the damping in the steady-state response of a building during soil–structure interaction. The building has been modelled by a single-degree-of-freedom system with rotational stiffness and with a viscous damper, placed on a circular foundation embedded into an elastic homogeneous half-space. The analysis is linear.

The system damping has been measured from the transfer function between the relative building response and the amplitude of the incident wave, using the analogy with the half-power method for a single-degree-of-freedom system with viscous damping. Both the dynamic and the kinematic interaction have been considered, for incident plante P- and SV-waves.

The effects of the following factors on the system damping ratio were studied: the height of the building relative to the width of the base, the mass of the building relative to the mass of the foundation and the mass of the replaced soil, the damping in the building, the relative stiffness of the building compared with the soil, the depth of the embedment, and the type of incident waves and their angle of incidence. Incident plane P- and SV-waves were considered.

We found many trends and features of our model to be in agreement with what has been known about soil–structure interaction for many years. Many of these trends are discussed in the above text and need not be repeated here. The important and new contributions of our work lie in the quantitative description of the system damping ratio, which results only from wave scattering and radiation from the rigid foundation in the

simple model studied here. Also, the analytical nature of our solution, and the simplicity of our model, should serve as useful calibration cases for more general numerical methods which are currently being developed by others.

Under favourable conditions, the system damping ratio (corresponding to, say, the first mode of the response of a tall building) can take on large values (in some cases in excess of 0·1), while the system is vibrating in the linear range of amplitudes. This suggests that, as designers of earthquake resistant strucutres, we should begin to look at a larger picture, trying to optimize also the overall system parameters, with the aim to reduce the relative building response. Clearly, this is not a simple problem, as it involves detailed understanding of the incident wave motion. However, at this time, when much effort is devoted to base isolation of structures, and towards active control of structural response, it would seem wise not to ignore the advantages which are already at our disposal, and are a part of the building environment, but which tend to be ignored or excluded by the simplistic design approach. Clearly, it is better to divert than to counteract the incident energy of strong earthquake ground motion. With this in mind, this paper can serve as a modest step in this direction, suggesting the conditions and the cases to be explored by more detailed three-dimensional and numerical models.

ACKNOWLEDGEMENT

The authors are indebted to the anonymous reviewers for the critical review and useful comments, which contributed to the clarity of this paper.

APPENDIX

List of frequently used symbols

β, μ, ν	shear wave velocity, shear modulus, and Poisson's ratio for the soil
h, a	depth and half-width of the foundation
ω, T	circular fequency and period of the incident wave
γ	incident angle (angle between the direction of propagation of the incident wave and the normal to the half-space surface)
$\eta = \omega a/\pi\beta$ $= 2a/\beta T$	dimensionless frequency
H_{sb}, W_{sb}	height and width of a shear-beam building model
H, r_b	height and radius of gyration of the equivalent SDOF building model
K_b, C_b	rotational stiffness and viscous damping of the equivalent SDOF building model
ζ, ω_N	damping ratio and fixed-base natural frequency of the equivalent SDOF building model
m_b, m_f, m_s	mass per unit length in the y-direction of the building, of the foundation and of the soil replaced by the foundation
ρ_b, ρ_s	mass density of the building and of the soil
$\eta_N = \omega_N a/\pi\beta$	dimensionless stiffness parameter of the building relative to the soil
g	acceleration due to gravity
Δ, V, φ	horizontal and vertical displacements and rocking angle of point O on the foundation
ψ^{rel}, u_b^{rel}, v_b^{rel}	relative angle of rocking and relative horizontal and vertical displacements of the equivalent SDOF building model
u^{ff}	amplitude of the horizontal component of the free-field motion on the surface
η^{sys}, ζ^{sys}	system frequency and system damping ratio
η^{rig}, ζ^{rig}	limits of η^{sys}, ζ^{sys} when the stiffness of the building goes to infinity

REFERENCES

1. R. Betti, 'Dynamic soil structure interaction for long-span cable-supported bridges', *Ph.D. Dissertation* Department of Civil Engineering, University of Southern California, Los Angeles California, 1991.
2. J. Bielak, 'Dynamics of building–soil interaction', *Ph.D. Thesis*, California Institute of Technology, Pasadena, California, 1971.
3. J. Bielak, 'Dynamic behaviour of structures with embedded foundations', *Earthquake eng. struct. dyn.* **3**, 259–274 (1975).

4. J. Bielak, 'Modal analysis for building–soil interaction', *J. eng. mech. div. ASCE* **102**, 771–786 (1976).
5. J. E. Luco, 'Soil–structure interaction and identification of structural models', *Proc. ASCE specialty conf.* Knoxville, Tennessee (1980).
6. A. Mita and J. E. Luco, 'Impedance functions and input motions for embedded square foundations', *J. geotech. eng. ASCE* **115**, 491–503 (1989).
7. J. H. Rainer, 'Damping in dynamic structure–foundation interaction', *Can. geotech. j.* **12**, 13–22 (1975).
8. N.-C. Tsai, 'Modal damping for soil–structure interaction', *J.. eng. mech. div. ASCE* **100**, 323–341 (1974).
9. M. I. Todorovska, 'Effect of the depth of the embedment on the system response during building–soil interaction', *Soil dyn. earthquake eng.* (in press).
10. M. I. Todorovska and M. D. Trifunac, 'Analytical model for building–foundation–soil interaction', *Report No. CE 90-01*, Department of Civil Engineering, University of Southern California, Los Angeles, California, 1990.
11. M. I. Todorovska and M. D. Trifunac, 'Radiation damping during two-dimensional, in-plane building–soil interaction', *Report No. CE 91-01*, Department of Civil Engineering, University of Southern California, Los Angeles, California, 1991.
12. M. D. Trifunac, 'A note on rotational components of earthquake motions on ground surface for incident body waves', *Soil dyn. earthquake eng.* **1**, 11–19 (1982).